Reed-Solomon Coding as a Multipath Fading Countermeasure for PCM/FM Aeronautical Telemetry

Michael D. Rice and Daniel H. Friend
Department of Electrical and Computer Engineering
Brigham Young University
Provo, UT 84602
mdr(@ee.byu.edu

Abstract

This paper evaluates the use of Reed-Solomon error correcting codes as a countermeasure for the bursty errors caused by multipath fading seen in aeronautical telemetry channels. The tradeoff between code rate and interleaving depth is analyzed and an equation for predicting the code rate given a fixed burst length and interleaving depth is presented. Close agreement is found between predictions made by this equation and simulated results.

Introduction

A Reed-Solomon code defined over GF(2^m), the Galois Field of order 2^m, has a natural length of $N = 2^m - 1$ symbols, each symbol being composed of $\log_2(2^m) = m$-bits [1]. An (N, K) Reed-Solomon code accepts K m-bit information symbols and appends $N - K$ m-bit parity symbols to form an N m-bit symbol codeword. An (N, K) Reed-Solomon code can correct $t=\lfloor \frac{N-K}{2} \rfloor$ symbol errors in an N symbol block. Reed-Solomon codes are particularly effective against bursty data because they correct symbols which are several bits long regardless of how many bit errors there are within the symbol. Thus, correcting a single symbol in a Reed-Solomon code can correct a burst of m consecutive bit errors. On real aeronautical telemetry channels, errors occur in bursts. The result is that some codewords have more errors than the code can correct and a large number of the following codewords have no errors. The interleaver spreads out the burst so that there are more codewords with errors, but the number of errors in each codeword is small enough to be corrected.

Figure 1 is an illustration of an I x N block interleaver. Each row of the interleaver array holds an entire codeword. I is referred to as the degree of interleaving or interleaving depth and indicates the number of codewords across which the burst is being spread.

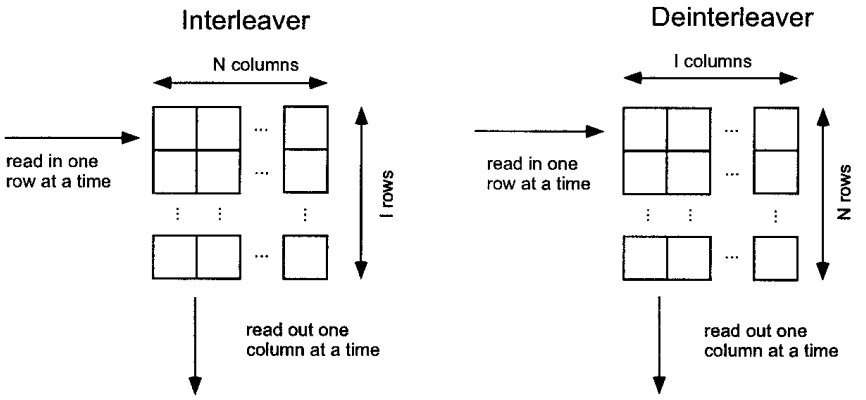

Figure 1: I x N Block Interleaver

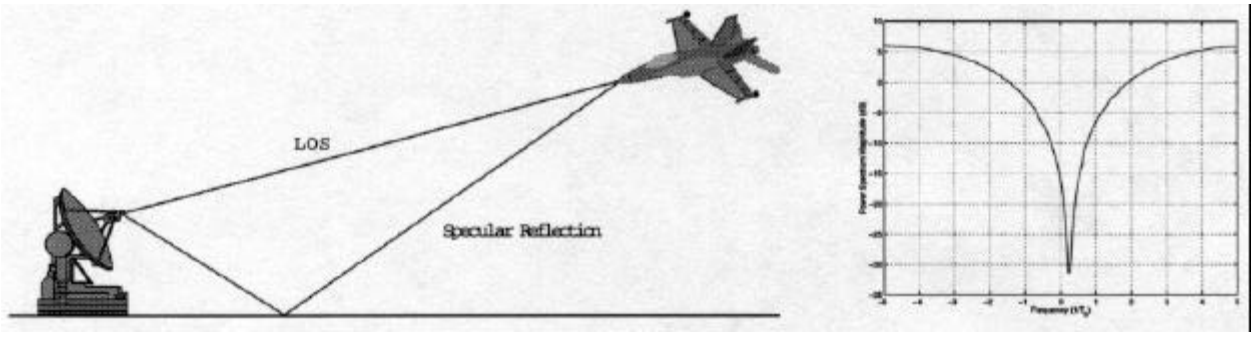

Figure 2: Multipath Channel Configuration and Plot of $|H(f)|^2$ for $\gamma = \gamma_0 - .05\pi$

Symbols are read into the interleaver in rows and then read out of the bottom of the interleaver by columns. A pair of symbols which were adjacent previous to being interleaved now have I symbols from $I - 1$ other codewords between them. In transmission, multipath fading causes a burst of symbol errors. Since the N symbols from a codeword are space I symbols apart by the interleaver, the burst causes a few errors in all the codewords rather than all the errors in a few codewords. At the de-interleaver, symbols are again read in by rows, this time of length I, and read out by columns of length N. This puts the data stream back into the original order.

There are costs associated with implementing error correction codes and interleaving data. To increase the number of errors a code can correct within a single codeword, K must be reduced. The result is a lower effective data rate, $\frac{K}{N}R_b$, where R_b is the bit rate. Decreasing K also increases the complexity of the hardware required to implement the code. Interleaving may reduce the code rate required to achieve a particular probability of bit error, but the cost is a non-zero delay equal to NmI/R_b seconds.

Effects of the Channel on the Transrnitted Signal

The PCM/FM aeronautical multipath channel is often modeled as the sum of a line-of-sight (LOS) signal and a single specular reflection as illustrated in Figure 2 [2, 3, 4]. The specular reflection differs in phase from LOS because of the time difference in path lengths, τ, and because of the phase shift imposed by the reflecting surface, γ. The reflecting surface also attenuates the specular component by an amount Γ. The equivalent complex baseband channel impulse response is [4]

$$h(t) = \delta(t) + \Gamma e^{j(2\pi f_0 \tau + \gamma)} \delta(t - \tau) \tag{1}$$

where f_0 is the PCM/FM carrier frequency. The squared magnitude of the Fourier transform of $h(t)$ is

$$|H(f)|^2 = 1 + \Gamma^2 + 2\Gamma \cos\left(2\pi(f - f_0)\tau + \gamma\right) \tag{2}$$

which has a null at

$$f = f_0 \pm \frac{1}{2\tau} - \frac{\gamma}{2\pi\tau} \tag{3}$$

as illustrated in Figure 2. Equation (3) shows the dependence of the location of the null on f_0, τ, and γ. As τ and γ vary during flight, the location of the null also varies. In many applications, γ varies constantly and at a rate much faster than τ changes so that the null appears to "sweep" through the PCM/FM spectrum from time to time. When the null is outside the signal bandwidth, transmissions remain error-free. However, when the null enters the signal bandwidth, errors occur at a very high rate. The result is long periods of error-free transmission interrupted by error bursts.

Let γ_0 be the phase difference which places the null in the center of the signal spectrum. Simulation results for unfiltered PCM/FM with frequency deviation of $0.35R_b$, $\Gamma = 0.99$, and $\Gamma / T_b = 0.1$ show that when γ is in the interval $(\gamma_0 - 0.32\pi, \gamma_0 + 0.32\pi)$ we see errors. This interval corresponds to null locations at frequencies $f_0 - 1.35R_b \le f \le f_0 + 1.35R_b$. Suppose the null sweeps through the signal spectrum at a rate of R_S Hz/sec. This will produce an error burst of length

$$x = \frac{2.7R_b}{R_S} R_b \text{ bits} \tag{4}$$

Code Rate Analysis

While the null is present within the bandwidth of the signal, there is some average symbol error rate P_B. Let x represent the duration of the error burst as defined in Equation (4). The worst case scenario occurs when the errors are grouped in such a way that they are contained within a minimum number of codewords. Thus, a sweep duration x of less than Nm bits would occur entirely within a single codeword rather than at the end of one codeword and the beginning of the following codeword. Sweep durations of more than Nm bits would be contained within $[x / Nm]$ codewords rather than $[x / Nm] + 1$ codewords. This requires the code to correct a maximum amount of errors per codeword. For some degree of interleaving I, the average symbol error rate would be reduced to

$$P_I = \frac{x/m}{NI} P_B \tag{5}$$

assuming there is a single error burst within the I interleaved codewords. This assumption is based on observations made during tests conducted at Edwards AFB where error bursts were separated by long periods of error-free transmission. Equation (5) indicates that NI should always be greater than x/m symbols in order for interleaving to reduce the average symbol error rate. This coincides with intuition because for NI less than or equal to x/m, the burst is not being spread over any error-free codewords; thus the average symbol error rate is not being reduced.

The code has to correct an average of NP_I symbol errors per codeword after de-interleaving. In order to correct these errors, the error correcting capability, t, must be at least $[NP_I]$. Since a t-error correcting Reed-Solomon code has message length $K = \mathrm{N} - 2t$, the resulting code rate required for a given sweep rate and interleaving depth would be

$$R_C = \frac{K}{N} = \frac{N - 2\lceil NP_I \rceil}{N} \tag{6}$$

For a fixed sweep rate, this equation shows that the code rate approaches 1 as the interleaving depth approaches ∞.

For example, error bursts seen in [5] were on the order of 500,000 bits or more. Bursts of this length would either require a codeword longer than 500,000 bits with a very low code rate, or a high interleaving depth. Since codes of this length are impractical, it is reasonable to choose a moderate code length and adjust the interleaving depth to allow increased error correction. Using a length 255 8-bit symbol Reed-Solomon code on a

10 Mbps channel, a code rate of 1/2 would require an interleaving depth of approximately $I = 550$ with a resulting delay of about 100 ms in order to correct a burst of 500,000 bit errors. Doubling the interleaving depth to $I = 1100$ would increase the code rate to 0.75 while also doubling the interleaving delay.

The effect of the code rate is to reduce the actual data rate of the channel. Suppose a 1 Mbps data rate is specified for data transmission. If the code rate is 1/2, this means that the channel would actually have to operate at 2 Mbps since only 1/2 of the bits in each transmitted codeword are information and the rest are used for the m-bit parity symbols. This code rate doubles the required bandwidth of the channel. To transmit 1 Mbps of information over a channel with a code rate of 1/10, the channel would have to operate at 10 Mbps. Thus, increasing the error correction capability of a code which as a result decreases the code rate has the effect of expanding the required channel bandwidth by a factor of $1/R_C$. Another option is to fix the code rate at some acceptable level, possibly determined by bandwidth limitations, and adjust the interleaving depth so that t is sufficient to correct the number of errors per codeword after de-interleaving. As stated previously, increasing I causes a non-zero delay of NMI/R_b seconds. Thus, there is a trade-off between required bandwidth and the delay introduced by interleaving. This tradeoff is illustrated in Figure 3 where $R_b = 10$ Mbps and bandwidth is $1.78R_b$ as defined in [6] for NRZ PCM/FM data with no premodulation filter and frequency deviation of $0.35R_b$. This figure shows that in order to reduce the required bandwidth the amount of delay must increase and vice versa.

Simulation Analysis

In simulations conducted for this paper, the specular reflection had constant differential path delay $\tau = 10$ ns, attenuation factor $\Gamma = 0.99$, and a linearly increasing phase γ. The bit rate was normalized to $R_b = 10$Mbps. A linear sweep was chosen to correspond with multipath fading as seen in a spectrum analyzer output recorded during an F-16 test flight at Edwards AFB [5, 7]. White Gaussian noise was also added to the channel so that the SNR was 12 dB yielding a bit error rate of less than 10^{-6}. Simulations were conducted at complex baseband using a length 255 Reed-Solomon code and byte-symbol block interleaving. Figure 4 shows a block diagram of the simulated transmitter, channel, and receiver. Figure 5 plots simulation results versus those predicted by Equation (6) for a sweep rate of 27 GHz/sec and $P_B = 0.56$. It is evident from Figure 5 that the code rate is asymptotically approaching 1 as the interleave depth increases toward ∞. This agrees with the behavior of Equation (6).

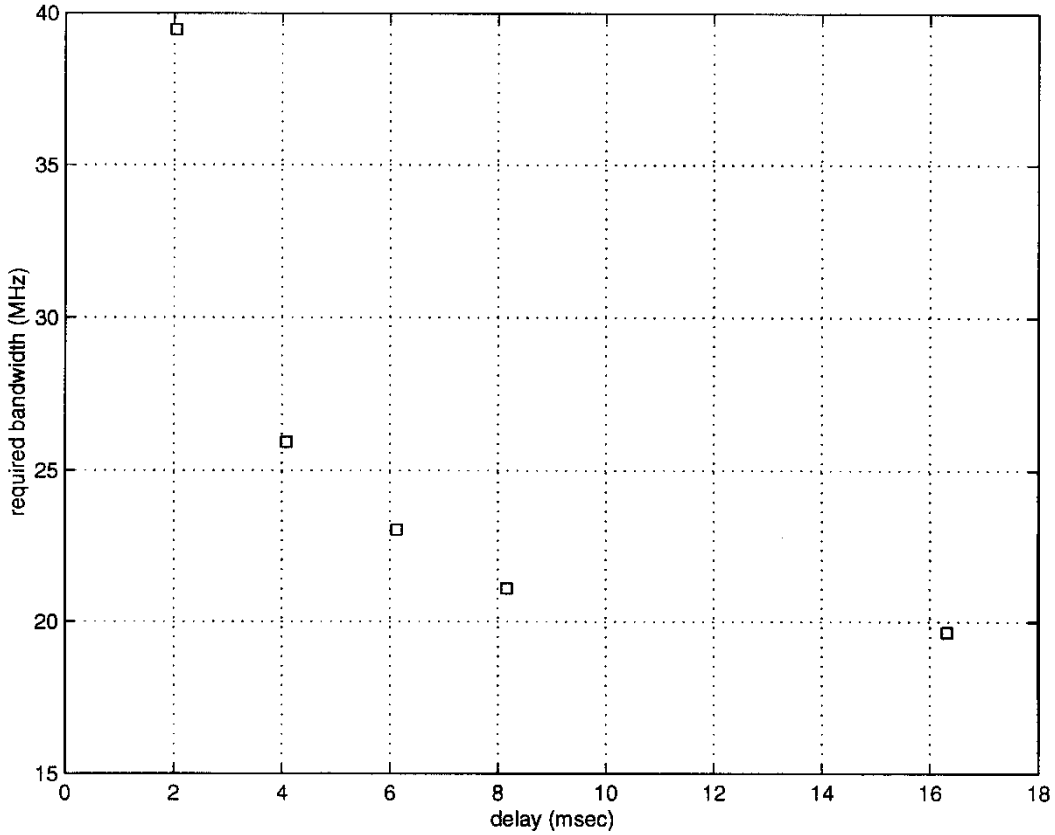

Figure 3: Bandwidth Expansion vs Interleaving Delay for Sweep Rate of 27 GHz/sec

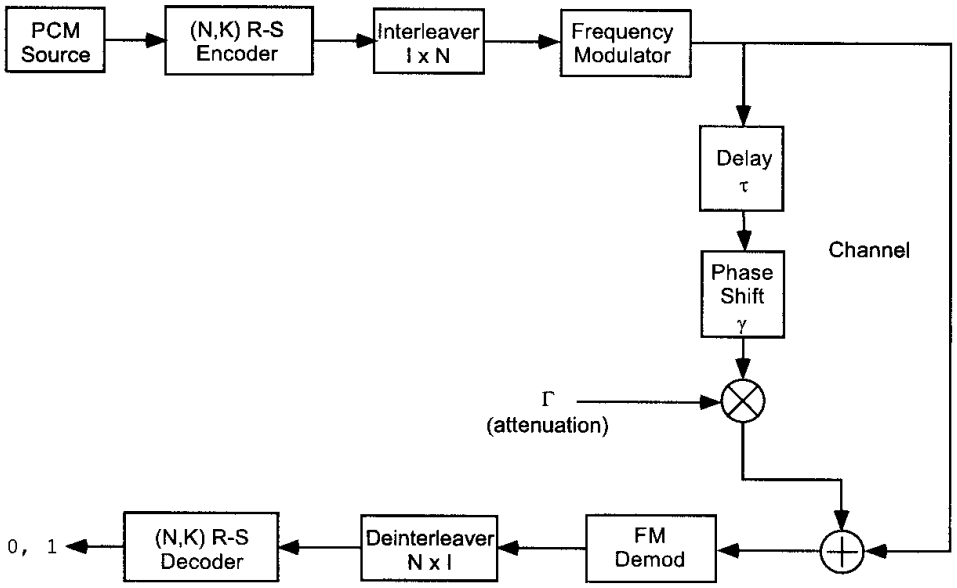

Figure 4: Block Diagram of PCM/FM Aeronautical Communication System

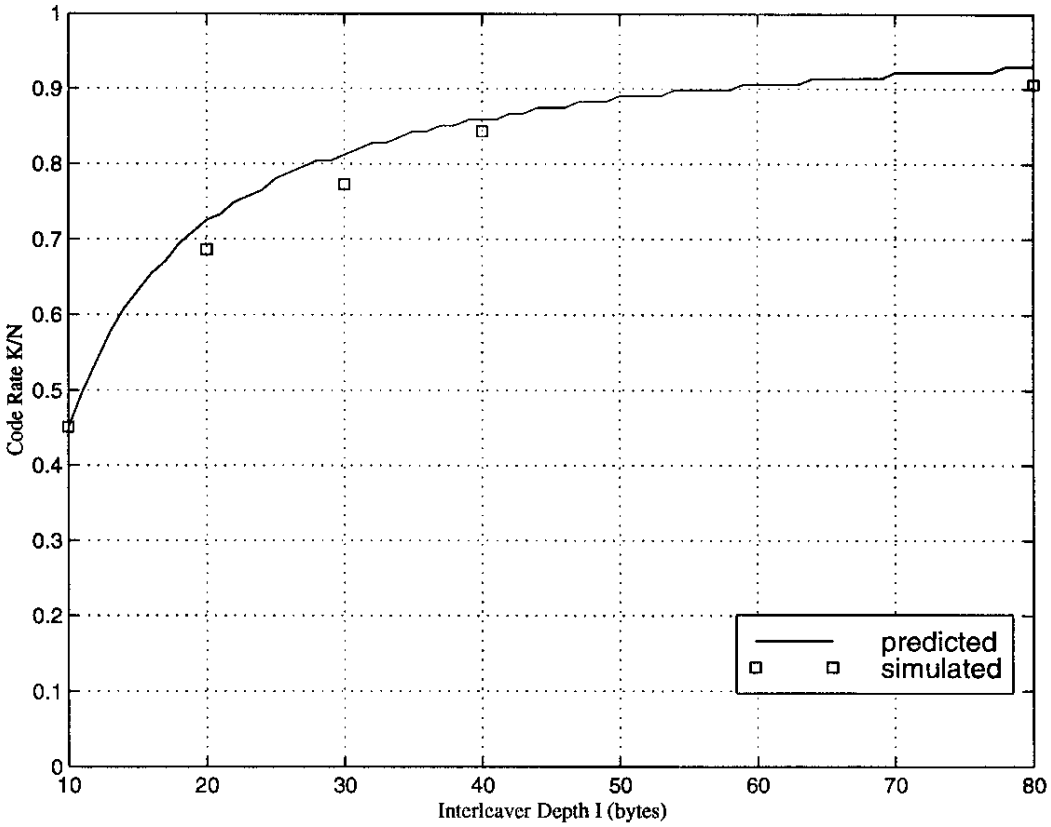

Figure 5: Simulated vs Predicted Code Rates for Sweep Rate of 27 GHz/sec

Conclusions

It is evident from Figure 5 that there is close agreement between the code rates predicted by equation 6 and simulation results. The small differences between predicted and simulated results can be attributed to the fact that the symbol error rate is a random variable and therefore deviates from its average value. Also, Figure 3 demonstrates the trade-off between required bandwidth and interleaving delay. Code rates close to 1 use the channel bandwidth more efficiently because the majority of bits transmitted actually represent information, but longer interleaving delays are required to achieve these code rates. As the amount of delay is decreased, the required channel bandwidth grows. Since code lengths greater than 255 bytes are beyond what is commercially available, error bursts of lengths such as those seen in [5] must be handled with longer interleaving depths rather than longer codewords. In applications where the bandwidth is fixed and very little of this bandwidth can be sacrificed due to a code rate much less than 1, we are forced to deal with some non-zero delay due to interleaving.

REFERENCES

[1] Stephen B. Wicker. *Error Control Systems for Digital Communication and Storage*. Prentice Hall, Englewood Cliffs, NJ, 1995.

[2] N. Tom Nelson. Probability of bit error on a standard IRIG telemetry channel using the aeronautical fading channel model. In *Proceedings of the International Telemetering Conference*, volume 30, pages 356-363, October 1994.

[3] Lyman Horne and Ricky Dye. Parameter characterization on a telemetry channel including the effects of the specular ray. In *Proceedings of the International Telemetering Conference*, volume 31, pages 210-215, October 1995.

[4] Michael Rice and Gene Law. Aeronautical telemetry fading sources at test ranges. In *Proceedings of the International Telemetering Conference*, volume 33, October 1997.

[5] Daniel Friend. BER analysis of an F-16 test run at Edwards AFB. In *Proceedings of the International Telemetering Conference*, volume 33, October 1997.

[6] Range Commanders Council Telemetry Group. *Telemetry Standards*. U.S. Army White Sands Missile Range, NM, irig standard 106-96 edition, May 1996.

[7] John Reddemann. Edwards range telemetry evaluation. In *International Test and Evaluation Conference, Lancaster*, CA, April 1997.